Inorg. Chem. **2006**, *45*, 1124–1129

Incorporation of Triazacyclononane into the Metal Phosphonate Backbones

Song-Song Bao, Gang-Sheng Chen, Yin Wang, Yi-Zhi Li, Li-Min Zheng,* and Qin-Hui Luo

State Key Laboratory of Coordination Chemistry, Coordination Chemistry Institute, Nanjing University, Nanjing 210093, P. R. China

Received September 1, 2005

This paper reports the syntheses and crystal structures of a manganese and a uranyl phosphonate based on 1,4,7-triazacyclononane-1,4,7-triyl- tris(methylenephosphonic acid), namely, $Mn_3\{C_9N_3H_{18}(PO_3)_3\}(H_2O)_6\cdot 1.5H_2O$ (**1**) and $UO_2\{C_9N_3H_{19}(PO_3H)_3\}\cdot H_2O$ (**2**). Compound **1** shows a unique layer structure where the hydrophobic triazacyclononane moieties all reside on one side of the inorganic backbone of the manganese phosphonate layer while the hydrophilic coordinated water molecules reside on the other side. In compound **2**, the triazacyclononane moieties are immobilized on the inorganic backbone of the uranyl phosphonate chains. The magnetic properties of compound **1** and the ion exchange properties of compound **2** have been studied.

Introduction

The immobilization of macrocycles on polymeric supports is of great interest because of their wide applications in such areas as separation, ion transportation, isotope extraction, sensoring, catalysis, etc.[1] Metal phosphonates are a class of hybrid materials that can integrate organic and inorganic characteristics within a single molecular composite.[2] Macrocycles functionalized by phosphonate groups may react with metal salts, yielding materials that bear macrocycle properties in association with robust inorganic backbones. Recent work has indicated that crown ethers can be incorporated into zirconium phosphonate layers or other metal phosphonate networks.[3] Triaza- and tetraaza-macrocycles and their derivatives have been extensively studied because of their strong coordination capabilities toward metal ions.[4] For those with methylenephosphonate pendant arms, attention has been paid to the tetraazamacrocycles.[5] The complexation studies based on 1,4,7-triazacyclononane-1,4,7-triyl-tris(methylenephosphonic acid) [notpH_6, $C_9H_{18}N_3(PO_3H_2)_3$] (Scheme 1) were mainly carried out on their solution properties.[6] Only two compounds (e.g., Fe(notpH_3)[7] and Cu(notpH_4)$\cdot H_2O$)[8] have been structurally characterized so far. Both show simple mononuclear structures in which the Fe(III) ion is six coordinated, the Cu(II) ion is five coordinated, and part of the phosphonate oxygen atoms are protonated. Herein, we report two hybrid materials where the triazamacrocycles are immobilized on the metal phosphonate layers or chains, namely, $Mn_3\{C_9N_3H_{18}(PO_3)_3\}(H_2O)_6\cdot 1.5H_2O$ (**1**) and $UO_2\{C_9N_3H_{19}(PO_3H)_3\}\cdot H_2O$ (**2**).

Experimental Section

All chemicals and solvents were used as purchased. The notpH_6 was prepared by a modified literature method.[9] Elemental analyses

* To whom correspondence should be addressed. E-mail: lmzheng@netra.nju.edu.cn. Fax: +86−25−83314502.

(1) (a) Gokel, G. W. *Chem. Soc. Rev.* **1992**, *21*, 39. (b) Chuit, C.; Corriu, R. J. P.; Dubois, G.; Reye, C. *Chem. Commun.* **1999**, 723. (c) Alexandratos, S. D.; Natesan, S. *Ind. Eng. Chem. Res.* **2000**, *39*, 3998. (d) Gasparrini, F.; Misiti, D.; Pierini, M.; Villani, C. *Org. Lett.* **2002**, *4*, 3993. (e) Dumaine-Bouaziz, M.; Cordier, D.; Morelis, R. M.; Coulet, P. R. *Langmuir* **1997**, *13*, 5711. (f) Poltowicz, J.; Haber, J. *J. Mol. Catal. A* **2004**, *220*, 43.

(2) (a) Alberti, G. In *Comprehensive Supramolecular Chemistry*; Lehn, J. M. Ed.; Pergamon: Oxford, U.K., 1996; Vol. 7. (b) Cao, G.; Hong, H.; Mallouk, T. E. *Acc. Chem. Res.* **1992**, *25*, 420. (c) Clearfield, A. *Prog. Inorg. Chem.* **1998**, *47*, 371.

(3) (a) Zhang, B.; Clearfield, A. *J. Am. Chem. Soc.* **1997**, *119*, 2751. (b) Sharma, C. V. K.; Clearfield, A. *J. Am. Chem. Soc.* **2000**, *122*, 1558. (c) Ngo, H. L.; Lin, W. *J. Am. Chem. Soc.* **2002**, *124*, 14298.

(4) (a) Bernhardt, P. V.; Lawrance, G. A. *Coord. Chem. Rev.* **1990**, *104*, 297. (b) Hancock, R. D.; Maumela, H.; De Sousa, A. S. *Coord. Chem. Rev.* **1996**, *148*, 315. (c) Wainwright, K. P. *Coord. Chem. Rev.* **1997**, *166*, 35.

(5) (a) Lukes, I.; Kotek, J.; Vojtisek, P.; Hermann, P. *Coord. Chem. Rev.* **2001**, *216−217*, 287. (b) Kotek, J.; Lubal, P.; Hermann, P.; Cisarova, I.; Lukes, I.; Godula, T.; Svobodova, I.; Taborsky, P.; Havel, J. *Chem.—Eur. J.* **2003**, *9*, 233. (c) Kong, D.; Medvedev, D. G.; Clearfield, A. *Inorg. Chem.* **2004**, *43*, 7308.

(6) Prata, M. I. M.; Santos, A. C.; Geraldes, C. F. G. C.; de Lima, J. J. P. *J. Inorg. Biochem.* **2000**, *79*, 359.

(7) Yu Antipin, M.; Baranov, A. P.; Kabachnik, M. I.; Ya Medved, T.; Polikarpov, Yu. M.; Struchkov, Yu. T.; Shcherbakov, B. K. *Dokl. Akad. Nauk SSSR (Russ.) (Proc. Nat. Acad. Sci. USSR)* **1986**, *287*, 130.

(8) Kabachnik, M. I.; Yu Antipin, M.; Shcherbakov, B. K.; Baranov, A. P.; Struchkov, Yu. T.; Ya Medved, T.; Polikarpov, Yu. M. *Koord. Khim. (Russ.) (Coord. Chem.)* **1988**, *14*, 536.

10.1021/ic051498e CCC: $33.50
Published on Web 01/07/2006

Scheme 1

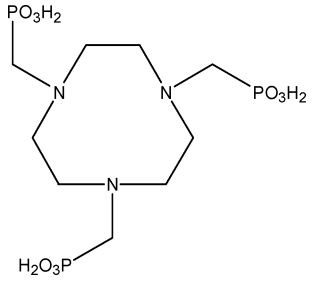

were performed on a Perkin-Elmer 240C elemental analyzer. The IR spectra were obtained as KBr disks on a VECTOR 22 spectrometer. Thermal analysis was performed in nitrogen in the temperature range of 50−800 °C with a heating rate of 10 °C/min on a TGA-DTA V1.1b Inst 2100 instrument. The powder XRD patterns were recorded on a Shimadzu XD-3A X-ray diffractometer. The metal analyses were carried out in an ARL-9800 X-ray fluorescence spectrometer. Variable-temperature magnetic susceptibility data were obtained on microcrystalline samples (34.41 mg for compound **1** and 8.10 mg for the dehydrate form of **1**) from 1.8 to 300 K in a magnetic field of 2 kOe, using a Quantum Design MPMS-XL7 SQUID magnetometer. Diamagnetic corrections were estimated from Pascal's constants.[10]

$Mn_3\{C_9N_3H_{18}(PO_3)_3\}(H_2O)_6\cdot 1.5H_2O$ (1). A mixture of $Mn(OAc)_2\cdot 4H_2O$ (0.15 mmol, 0.037 g), notpH_6 (0.05 mmol, 0.022 g), and H_2O (8 cm^3), adjusted with 1 M $NH_3\cdot H_2O$ to pH 5.0, was heated in a Teflon-lined autoclave at 140 °C for 72 h. Hexagonal sheetlike colorless crystals were obtained as a monophasic material with a yield of 70% (based on Mn). IR (KBr, cm^{-1}): 3417(s), 2939(m), 2915(m), 2861(m), 2831(m), 1673(m), 1469(w), 1463(w), 1374(w), 1319(w), 1293(w), 1169(m), 1095(s), 1055(s), 1029(s), 998(s), 958(m), 783(w), 750(w), 583(m), 453(w). Anal. Calcd for $C_9H_{33}N_3P_3O_{16.5}Mn_3$: C, 15.32; H, 4.68; N, 5.96. Found: C, 14.84; H, 4.65; N, 6.14.

$UO_2\{C_9N_3H_{19}(PO_3H)_3\}\cdot H_2O$ (2). A mixture of $UO_2(OAc)_2$ (0.025 mmol, 0.0097 g), notpH_6 (0.05 mmol, 0.022 g), H_2O (8 cm^3), and 1 M HCl (0.3 cm^3) (pH 1.2) was hydrothermally treated at 140 °C for 12 h. Taperlike yellow crystals were obtained as a monophasic material with a yield of 82% (based on U). IR (KBr, cm^{-1}): 3650(w), 3530(w), 3173(w), 2857(br), 1606(w), 1487(w), 1461(w), 1377(w), 1303(w), 1262(m), 1154(s), 1085(s), 999(s), 948(s), 899(s), 773(m), 549(m), 455(br). Anal. Calcd for $C_9H_{24}N_3O_{12}P_3U$: C, 15.49; H, 3.44; N, 6.02. Found: C, 15.09; H, 3.94; N, 6.16.

Crystallographic Studies. Single crystals of dimensions 0.20 × 0.20 × 0.05 mm^3 for **1** and 0.22 × 0.12 × 0.05 mm^3 for **2** were selected for indexing and intensity data collection on a Bruker SMART APEX CCD diffractometer using graphite-monochromated Mo Kα radiation (λ = 0.71073 Å) at room temperature. The numbers of collected and observed independent [$I > 2\sigma(I)$] reflections are 6500 and 1205 (R_{int} = 0.064) for **1** and 9643 and 2933 (R_{int} = 0.036) for **2**. The data were integrated using the Siemens SAINT program.[11] Absorption corrections were applied. The structures were solved by direct methods and refined on F^2 by full-matrix least-squares using SHELXTL.[12] Crystallographic and refinement details are listed in Table 1 with selected bond lengths and angles in Tables 2 and 3.

Table 1. Crystallographic Data for Compound **1**

	1	**2**
formula	$Mn_3C_9H_{33}N_3O_{16.5}P_3$	$C_9H_{24}N_3O_{12}P_3U$
M	705.10	697.25
cryst syst	trigonal	monoclinic
space group	$R\bar{3}$	$P2_1/c$
a (Å)	9.3049(14)	11.818(7)
b (Å)	9.3049(14)	11.355(7)
c (Å)	47.880(11)	14.866(9)
β (deg)		112.052(11)
V ($Å^{-3}$)	3590.1(11)	1848.9(19)
Z	3	4
D_c (g cm^{-3})	1.957	2.505
F(000)	1080	1328
GOF on F^2	1.033	1.084
R_1, $R_2[I > 2\sigma(I)]$	0.0516, 0.1025	0.0530, 0.1171
R_1, R_2(all data)	0.0709, 0.1058	0.0685, 0.1219
$(\Delta\rho)_{max}$, $(\Delta\rho)_{min}$ (e $Å^{-3}$)	0.460, −0.759	1.811, −2.747

Table 2. Selected Bond Lengths (Å) and Angles (deg) for Compound **1**[a]

Mn(1)−O(1)	2.110(3)	Mn(1)−N(1)	2.334(3)
Mn(2)−O(2)	2.121(3)	Mn(2)−O(1W)	2.271(3)
Mn(3)−O(3)	2.104(3)	Mn(3)−O(2W)	2.198(3)
P(1)−O(1)	1.540(3)	P(1)−O(2)	1.511(3)
P(1)−O(3)	1.519(3)		

O(1A)−Mn(1)−O(1)	98.6(1)	O(1)−Mn(1)−N(1B)	156.8(1)
O(1)−Mn(1)−N(1A)	104.4(1)	O(1)−Mn(1)−N(1)	81.5(1)
N(1A)−Mn(1)−N(1)	76.1(1)	O(2)−Mn(2)−O(2C)	97.6(1)
O(2)−Mn(2)−O(1W)	168.3(1)	O(2C)−Mn(2)−O(1W)	88.7(1)
O(2D)−Mn(2)−O(1W)	91.3(1)	O(1W)−Mn(2)−O(1WC)	81.3(1)
O(3E)−Mn(3)−O(3)	97.5(1)	O(3)−Mn(3)−O(2WF)	165.0(1)
O(3)−Mn(3)−O(2WE)	85.6(1)	O(3)−Mn(3)−O(2W)	96.6(1)
O(2WE)−Mn(3)−O(2W)	79.5(1)	P(1)−O(1)−Mn(1)	121.4(1)
P(1)−O(2)−Mn(2)	126.9(2)	P(1)−O(3)−Mn(3)	154.5(2)
C(3)−N(1)−Mn(1)	104.7(2)	C(2)−N(1)−Mn(1)	110.6(2)
C(1)−N(1)−Mn(1)	106.5(2)		

[a] Symmetry transformations used to generate equivalent atoms: A $-y+1, x-y, z$; B $-x+y+1, -x+1, z$; C $-y, x-y, z$; D $-x+y, -x, z$; E $-x+y, -x+1, z$; F $-y+1, x-y+1, z$.

Results and Discussion

Syntheses. Compounds **1** and **2** have been synthesized by the reactions of $Mn(OAc)_2\cdot 4H_2O$ or $UO_2(OAc)_2$ with notpH_6 under hydrothermal conditions. Many factors may affect both the composition and morphologies of the final products including the pH, molar ratio of the starting materials and different metal sources, etc. Compound **1** is obtained when the pH of the reactant mixture (molar ratio $Mn(OAc)_2$/notpH_6 = 3:1) is adjusted by $NH_3\cdot H_2O$ to 5.0−6.0. At a lower pH (1.0−4.5), only a clear solution is observed. A higher pH (6.0−8.0) promotes the formation of a mixture of white and brown precipitates. Different molar ratios of the starting materials ($Mn(OAc)_2$/notpH_6 = 1:1, 2:1) under the same reaction conditions with pH 5.0−6.0 leads to the same crystalline material but with a lower yield. If NaOH instead of $NH_3\cdot H_2O$ is used to adjust the pH value, a white powder phase of **1** results as determined from the the powder XRD patterns. The replacement of $Mn(OAc)_2$ by the other manganese salts ($MnCl_2$ or $MnSO_4$) produces compound **1** in the form of both crystalline and powder phases.

Single crystals of compound **2** with a good yield can be obtained when the molar ratio of $UO_2(OAc)_2$/notpH_6 is 1:2

(9) (a) Wieghard, K.; Schmid, W.; Nuber, B.; Weiss, J. *Chem. Ber.* **1979**, *112*, 2220. (b) Atkins, T. J.; Richman, J. E.; Oettle, W. F. *Org. Synth.* **1978**, *58*, 87.
(10) Kahn, O. *Molecular Magnetism*; VCH Publishers: New York, 1993.
(11) *SAINT, Program for Data Extraction and Reduction*, version 6.01; Siemens Analytical X-ray Instruments Inc.: Madison, WI.
(12) Sheldrick, G. M. *SHELXTL, Program for Refinement of Crystal Structures*, version 6.10; Siemens Analytical X-ray Instruments Inc.: Madison, WI.

Table 3. Selected Bond Lengths (Å) and Angles (deg) for Compound **2**[a]

U(1)−O(10)	1.769(8)	U(1)−O(11)	1.792(7)
U(1)−O(5A)	2.308(8)	U(1)−O(4B)	2.332(8)
U(1)−O(8C)	2.350(9)	U(1)−O(1)	2.374(8)
U(1)−O(7A)	2.408(7)	P(1)−O(1)	1.481(8)
P(1)−O(2)	1.511(8)	P(1)−O(3)	1.582(7)
P(2)−O(4)	1.533(8)	P(2)−O(5)	1.500(8)
P(2)−O(6)	1.554(9)	P(3)−O(7)	1.499(8)
P(3)−O(8)	1.500(9)	P(3)−O(9)	1.528(8)
O(10)−U(1)−O(11)	178.7(4)	O(10)−U(1)−O(5A)	87.6(4)
O(11)−U(1)−O(5A)	93.2(3)	O(10)−U(1)−O(4B)	89.7(3)
O(11)−U(1)−O(4B)	89.0(3)	O(5A)−U(1)−O(4B)	145.9(3)
O(10)−U(1)−O(8C)	96.6(4)	O(11)−U(1)−O(8C)	84.7(3)
O(5A)−U(1)−O(8C)	70.6(3)	O(4B)−U(1)−O(8C)	143.4(3)
O(10)−U(1)−O(1)	87.8(3)	O(11)−U(1)−O(1)	92.3(3)
O(5A)−U(1)−O(1)	139.3(3)	O(4B)−U(1)−O(1)	74.4(3)
O(8C)−U(1)−O(1)	69.9(3)	O(10)−U(1)−O(7A)	94.0(3)
O(11)−U(1)−O(7A)	85.2(3)	O(5A)−U(1)−O(7A)	72.6(3)
O(4B)−U(1)−O(7A)	73.7(2)	O(8C)−U(1)−O(7A)	141.1(3)
O(1)−U(1)−O(7A)	148.0(3)	P(1)−O(1)−U(1)	142.7(5)
P(2)−O(4)−U(1B)	144.8(4)	P(2)−O(5)−U(1D)	177.6(6)
P(3)−O(7)−U(1D)	144.5(5)	P(3)−O(8)−U(1C)	154.1(5)

[a] Symmetry transformations used to generate equivalent atoms: A $x+1, -y+3/2, z+1/2$; B $-x+1, -y+1, -z+1$; C $-x+1, -y+2, -z+1$; D $x-1, -y+3/2, z-1/2$.

and the pH value of the mixture is adjusted to 1.1−1.6. When the pH is lower than 1.0, a clear solution is observed together with very few crystals floating on the top of the solution. If pH is higher (1.7−7.0), a yellow floccule of **2** would be produced as recognized by their XRD patterns (see Supporting Information). Reactions with other molar ratios of $UO_2(OAc)_2$/notpH_6 (1:1, 2:1) were also studied, but they resulted in the yellow powder or floccule phases of **2** at the same pH (1.1−7.0), determined by their XRD patterns. Clearly, the pH plays an important role not only in producing pure phases of **1** and **2** but also in the crystallization of these products.

We have also studied the hydrothermal reactions of notpH_6 with many other transition metal (Cr, Fe, Co, Ni, Cu, Zn) salts or lanthanide sources. Unfortunately, only powder phases or clear solutions are obtained under similar conditions. The powder X-ray diffraction analyses reveal that the structures of these powder phases are different from those of **1** and **2**.

Structure of $Mn_3\{C_9N_3H_{18}(PO_3)_3\}(H_2O)_6\cdot 1.5H_2O$ (1). Complex **1** crystallizes in a high-symmetrical trigonal space group $R\bar{3}$. The structure results from the three crystallographically unique Mn atoms that are bridged by nine phosphonate oxygen atoms of the notp^{6-} ligand to yield a two-dimensional structure in the *ab* plane containing 12-membered rings (Figures 1 and 2). Each of the three Mn atoms in **1** locates at a C_3 axis and has a distorted octahedral geometry. The Mn(1) atom is wrapped by two sets of facial donors from the same notp^{6-} group (i.e., three macrocyclic nitrogen atoms [N(1), N(1A), N(1B)] on one hand and three pendant phosphonate oxygens [O(1), O(1A), O(1B)] on the other). The resulting Mn(notp)$^{4-}$ unit serves as a second building block and further links the Mn(2) and Mn(3) atoms through the remaining two phosphonate oxygens [O(2), O(3)] of each {CPO_3} terminus. Thus, one facial position of each {Mn(2)O_6} or {Mn(3)O_6} octahedron is occupied by three

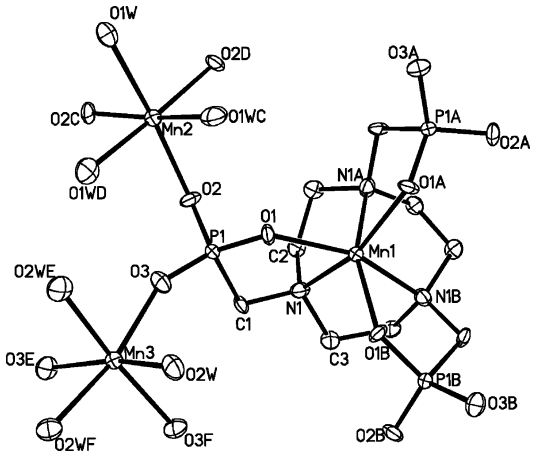

Figure 1. Building unit of structure **1** with the atomic labeling scheme. Thermal ellipsoids are at the 50% probability.

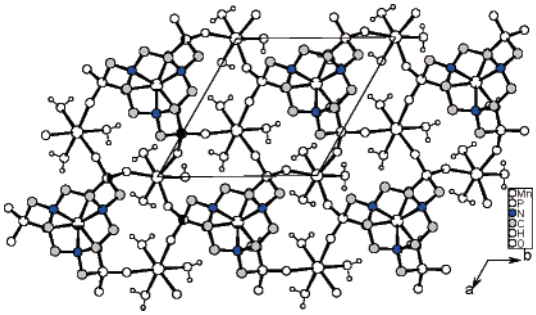

Figure 2. One layer of structure **1**. All H atoms except those of H_2O are omitted for clarity.

equivalent O(2) or O(3) atoms, respectively, while the other facial positions are filled with water molecules. The Mn−N distances (2.340(3) Å) and the N−Mn−N bond angles (76.4(1)°) are in agreement with those in compound [{Mn(dmptacn)(CN)}$_6$Cr][Cr(CN)$_6$](ClO$_4$)$_6\cdot 6H_2O$[13] (dmptacn = 1,4-bis(2-methyl-pyridyl)-1,4,7-triazacyclononane) (Mn−N = 2.236(5)−2.316(4) Å, N−Mn−N = 75.4(1)−76.7(2)°). The Mn−O bond lengths (2.107(3)−2.280(3) Å) and the O−Mn−O (86.9(1)−170.1(1)°) and O−Mn−N bond angles (156.6(1)°) may be compared to those in Fe(notpH_3)[7] (1.944 Å, 99.20°, and 83.81−163.39°) and Cu(notpH_4)$\cdot H_2O$[8] (1.936 Å, 90.66°, and 89.17−168.16°).

The notp^{6-} anion contains three equivalent CPO_3 termini, each of which coordinates to three different Mn atoms through three phosphonate oxygens [O(1), O(2), O(3)], thereby leading to a two-dimensional architecture (Figure 2). The Mn···Mn distances over the O−P−O bridges within the layer are 5.438 Å for Mn(1)···Mn(2), 5.879 Å for Mn(1)···Mn(3), and 5.589 Å for Mn(2)···Mn(3). Compared with the other manganese phosphonates,[14] the layer structure of **1** is unusual in that the hydrophobic triazacyclononane moieties all reside on one side of the inorganic backbone of the manganese phosphonate layer while the hydrophilic coordinated water molecules all reside on the other side. As a

(13) Parker, R. J.; Spiccia, L.; Berry, K. J.; Fallon, G. D.; Moubaraki, B.; Murray, K. S. *Chem. Commun.* **2001**, 333.

(14) (a) Cao, G.; Lee, H.; Lynch, V. M.; Mallouk, T. E. *Inorg. Chem.* **1988**, *27*, 2781. (b) Cabeza, A.; Ouyang, X.; Sharma, C. V. K.; Aranda, M. A. G.; Bruque, S.; Clearfield, A. *Inorg. Chem.* **2002**, *41*, 2325. (c) Stock, N.; Bein, T. *Angew. Chem., Int. Ed.* **2004**, *43*, 749.

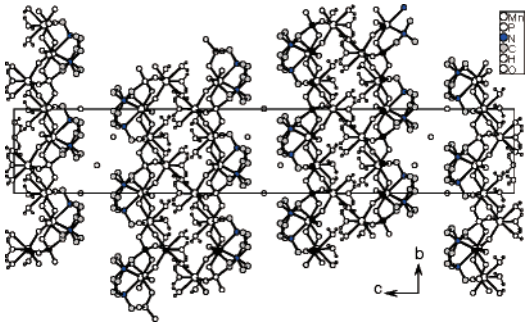

Figure 3. Packing diagram of structure **1** along the *a* axis. All H atoms except those of the coordinated H_2O molecules are omitted for clarity.

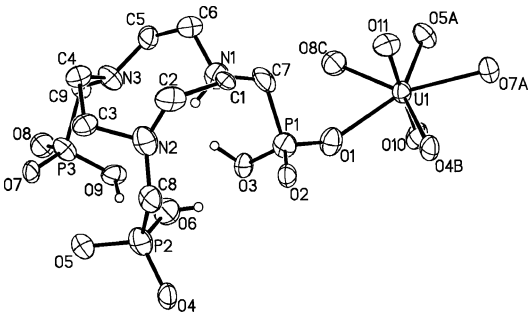

Figure 4. Building unit of structure **1** with the atomic labeling scheme. Thermal ellipsoids are at the 50% probability.

consequence, two hydrophilic sides of adjacent layers are attracted to each other through hydrogen bonds, resulting in a double layer with a "water reservoir" in the middle. Figure 3 clearly shows the stacking mode of these layers.

Structure of $UO_2\{C_9N_3H_{19}(PO_3H)_3\}\cdot H_2O$ (2). Complex **2** shows a different type of layer structure. The asymmetric unit of structure **2** consists of one uranyl unit, one notpH_4^{2-}, and one water molecule. Each uranyl unit is coordinated by five oxygen atoms in the equatorial plane to yield a $\{UO_7\}$ pentagonal bipyramid (Figure 4). The uranyl group is almost linear (O(10)−U−O(11) = 178.7(4)°) and the U=O distances are normal (1.769(8)−1.792(7) Å). The equatorial U−O distances (2.308(8)−2.408(7) Å) are in agreement with those in the other uranyl phosphonates.[15] The notpH_4^{2-} in **2** behaves as a zwitterion ligand with one triazamacrocyclic nitrogen atom [N(1)] and three phosphonate oxygen atoms [O(3), O(6), O(9)] being protonated (Figure 4). Five of the remaining six phosphonate oxygen atoms [O(1), O(4), O(5), O(7), O(8)] are involved in the coordination with the uranium atoms, leading to a two-dimensional layer (Figure 5). The remaining phosphonate oxygen [O(2)] is pendant. Within the layer, infinite chains composed of corner-sharing $\{UO_7\}$ pentagonal bipyramids and $\{CPO_3\}$ tetrahedra are found parallel to the *b* axis, which contain eight-member rings (Figure 5). This chain is strikingly similar to those observed for $[UO_2(HO_3PC_6H_5)_2(H_2O)]_2\cdot 8H_2O$, $UO_2(HO_3PC_6H_5)_2\cdot 2CH_3CH_2OH$,[15b] and $UO_2(HO_3PC_6H_5)_2(H_2O)\cdot 2H_2O$,[15c] although the overall structures of the latter complexes are one-dimensional. Accordingly, the layer in **2** can be viewed as inorganic chains of uranyl phosphonate well separated by the triazacyclononane moieties. It is noted that the layer also contains 22-member rings, composed of two uranium atoms and two notpH_4^{2-} groups. As shown in Figure 6, the protonated phosphonate oxygens [O(3), O(6), O(9)] form a hydrophilic cage together with the macrocyclic ring. Such cages could potentially accommodate suitable metal ions or allow for ion exchange between the protons and the metal ions. Figure 7 shows the stacking diagram of these layers in structure **2**.

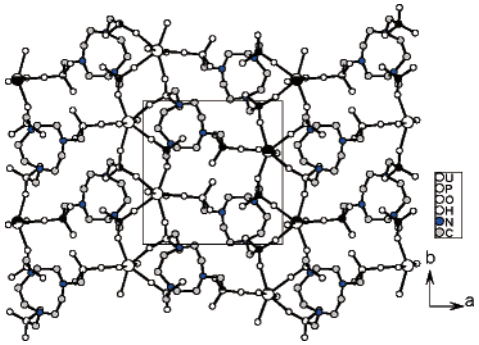

Figure 5. One layer of structure **1**. All H atoms are omitted for clarity.

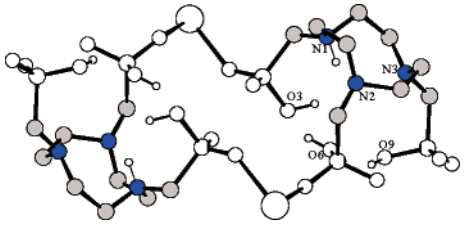

Figure 6. A 22-member ring within the layer of structure **1**.

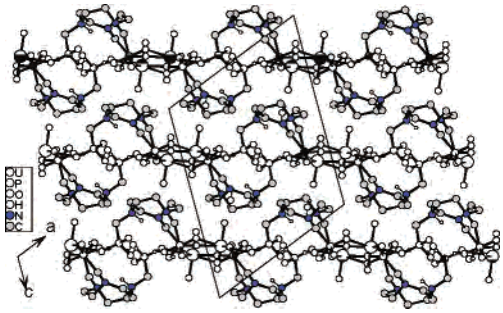

Figure 7. Packing diagram of structure **1** along the *b* axis. All H atoms are omitted for clarity.

It could be of interest to compare the different functions of the triazacyclononane in the two compounds. In **1**, the macrocyclic property of triazacyclononane is lost because of the coordination of all three nitrogen atoms to the Mn(II) ions. While in compound **2**, the protonated triazamacrocycles form hydrophilic cavities together with the protonated phosphonate oxygen donors. At first thought, one may conclude that it is a result of pH variation because the crystalline materials of compound **2** were obtained at a much lower pH (∼1.1−1.6) compared with those of compound **1** (pH ≈ 5−6). Nevertheless, our systematic work shows that compound **2** can also be obtained as a powder at a higher pH (1.7−7.0). Therefore, the differences in the functions of

(15) (a) Grohol, D.; Gingl, F.; Clearfield, A. *Inorg. Chem.* **1999**, *38*, 751. (b) Grohol, D.; Subramanian, M. A.; Poojary, D. M.; Clearfield, A. *Inorg. Chem.* **1996**, *35*, 5264. (c) Grohol, D.; Clearfield, A. *J. Am. Chem. Soc.* **1997**, *119*, 4662. (d) Doran, M. B.; Norquist, A. J.; O'Hare, D. *Chem. Mater.* **2003**, *15*, 1449. (e) Burns, P. C.; Ewing, R. C.; Hawthorne, F. C. *Can. Mineral.* **1997**, *35*, 1551.

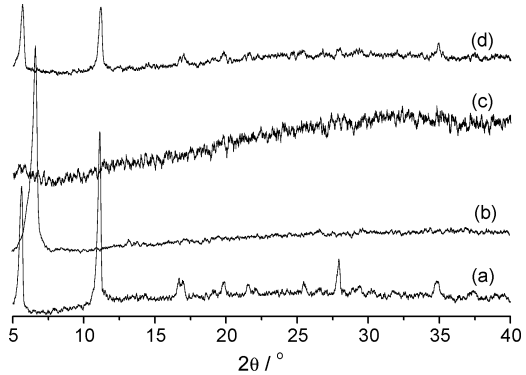

Figure 8. XRD patterns of compound **1** (a) before and (b) after dehydration, and those of the (c) the dehydrate form of **1** exposed to water vapor for 2 d or (d) refluxed at 100 °C for 4h.

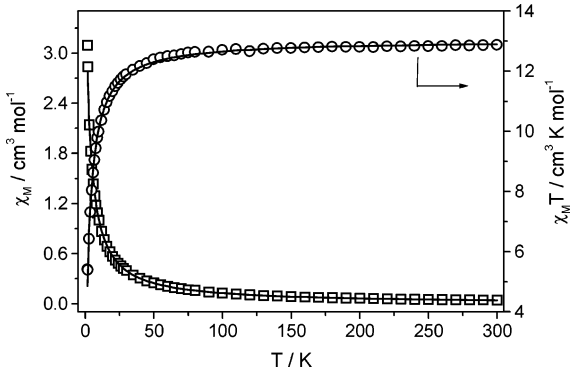

Figure 9. χ_M and $\chi_M T$ vs T plots for compound **1**.

the macrocycle in the present case are mainly caused by the different coordination capabilities of the manganese and uranyl cations. The latter prefers to coordinate with the oxygen donors, leaving the macrocycle nitrogen atoms free. These nitrogen atoms could be further protonated under acidic conditions.

Thermal Stability. The thermal analysis of **1** shows two steps of decomposition in the temperature range of 50−650 °C. The weight loss below 200 °C is 18.8%, in agreement with the removal of one and a half lattice waters and six coordinated water molecules (calcd 19.1%). Between 200 and 400 °C, the weight is nearly constant, indicating that a stable phase could be formed. Figure 8 gives the XRD patterns of complex **1** before and after the dehydration process. Clearly, a structural transformation occurs after dehydration. Such a transformation could be explained by the fact that the removal of the facial coordinated water molecules of the $\{Mn(2)O_6\}$ and $\{Mn(3)O_6\}$ octahedra would leave coordination vacancies for the metal ions which could be partly or fully occupied by the phosphonate oxygens from the neighboring layer. To examine the intercalation properties of the material, the dehydrate form of **1** was exposed to water vapor for 2 d. No distinct diffraction peaks, however, were observed, and the product became amorphous. When the dehydrate form was refluxed at 100 °C for 4h, compound **1** was recovered (Figure 8).

The thermal stability of **2** was also analyzed. The weight loss (2.1%) between 50 and 260 °C is close to the removal of lattice water molecule (calcd for $1H_2O = 2.6\%$). The XRD pattern of the dehydrate sample is the same as that of compound **2**. The sharp weight loss above 280 °C corresponds to the decomposition of the organic moieties and the collapse of the lattice.

Ion Exchange. To check the ion exchange properties of compound **2**, experiments were conducted by heating and stirring a mixture of **2** and 20 mL of 1 M $CaCl_2$ (0.1 M $CuCl_2$, 0.1 M $CoCl_2$, 0.1 M $NiSO_4$, or 0.1 M $Zn(NO_3)_2$] at 80 °C for 8 h. The pH values of the solutions before and after the exchange reactions are 9.38 and 4.89 for $CaCl_2$, 3.27 and 2.93 for $CuCl_2$, 4.90 and 3.28 for $CoCl_2$, 4.66 and 3.60 for $NiSO_4$, and 4.72 and 3.52 for $Zn(NO_3)_2$. The XFS measurements revealed that the molar ratios of the metal ions in the final products are 1:0.33 for U/Ca, 1:0.17 for U/Cu, 1:0.11 for U/Co, 1:0.14 for U/Ni, and 1:0.23 for U/Zn. The XRD patterns confirm that the original crystal structure of **2** is preserved in all cases. Structural determination was also performed for a Ca^{2+}-exchanged single crystal. The unit cell parameters, however, remained unchanged. The adsorption of the Ca^{2+} ions could occur on the surface of the crystalline material, as observed by Clearfield et al. in a Mn-DOTP (DOTP = 1,4,7,10-tetrakis(methylenephosphonic acid)-1,4,7,-10- tetraazacyclododecane) compound.[5c]

Magnetic Properties. The magnetic properties of compound **1** were investigated in the temperature range of 1.8−300 K (Figure 9). The effective magnetic moment per Mn_3 at 300 K is 10.19 μ_B, close to the theoretical value (10.25 μ_B) for three isolated Mn(II) ions ($S = 5/2$, $g = 2.0$). The susceptibility data obeys the Curie−Weiss law in the whole temperature range with a Weiss constant, θ, of −2.98 K. The decrease of $\chi_M T$ upon cooling also indicates a weak antiferromagnetic interaction between the magnetic centers. From the structure described above, two pathways are possible to mediate the magnetic exchanges: one is through the O−P−O bridges within the layer and the other is through the O−H···O hydrogen bonds between the layers. The data were thus analyzed by the expression for the 2D Heisenberg antiferromagnet of spin $S = 5/2$ based on the spin Hamiltonian, $H = -2J\sum S_i S_j$[16]

$$\chi_M = 2.91\frac{Ng^3\beta^2}{kT}\frac{1}{1 + 23.33x + 147.78x^2 + 405.48x^3 + 8171.3x^4 + 64968x^5 + 15811x^6}$$

where N is Avogadro's number, β is Bohr magneton, k is the Boltzmann constant, $2J$ is the exchange-coupling constant, and $x = J/kT$. Superexchanges between the layers (zJ') can be considered by the molecular field approximation, $\chi' = \chi/(1 - zJ'\chi)$. The theoretical fitting, shown as the solid line in Figure 9, gives $g = 1.99$, $2J = 1.9 \times 10^{-4}$ cm^{-1}, and $zJ' = -0.23$ cm^{-1}. The extremely small J value suggests that compound **1** is principally a paramagnetic system. For the dehydrate form of **1**, the Weiss constant, obtained by data in the temperature range of 50−300 K, becomes −22.06 K. The result demonstrates that the interlayer magnetic exchange is enhanced after the removal of the coordinated

(16) (a) Gil de Muro, I.; Mautner, F. A.; Insausti, M.; Lezama, L.; Arriortua, M. I.; Rojo, T. *Inorg. Chem.* **1998**, *37*, 3243. (b) Rushbrooke, G. S.; Wood, P. *J. Mol. Phys.* **1963**, *6*, 409.

water molecules. The enhancement could be the result of the the refilling of the coordination vacancies around the Mn(II) ions by the phosphonate oxygens from the neighboring layer.

Conclusion. The reactions of 1,4,7-triazacyclononane-1,4,7-triyl-tris(methylenephosphonic acid) with manganese or uranyl acetates under hydrothermal conditions have resulted in two novel complexes $Mn_3\{C_9N_3H_{18}(PO_3)_3\}(H_2O)_6\cdot 1.5H_2O$ (**1**) and $UO_2\{C_9N_3H_{19}(PO_3H)_3\}\cdot H_2O$ (**2**) showing unique layer structures. In the former case, the triazacyclononane moieties reside on one side of the inorganic backbone of the manganese phosphonate layer, while in the latter case they are located alternatively on two sides of the inorganic backbone of the uranyl phosphonate chain. Although the macrocyclic property is lost in **1** because of the coordination of all three nitrogen atoms to the Mn(II) ions, it is retained in compound **2** where the protonated triazamacrocycles form hydrophilic cavities together with the protonated phosphonate oxygen donors. Further work is in progress to prepare new phosphonate materials incorporating macrocycles and to study their chemical and physical properties.

Acknowledgment. We thank the NNSF of China (No. 20325103), the Ministry of Education of China and the NSF of Jiangsu province (No. BK2002078) for financial support, Mr. Yong-Jiang Liu for crystal data collections, and Dr. Y. Song for magnetic measurements.

Supporting Information Available: X-ray crystallographic files in CIF format for the two compounds, TG curves for the compounds, XRD patterns for compound **2**, χ_M and χ_M^{-1} versus T plots for compound **1**, and the XRD patterns of the products obtained at different pHs. This material is available free of charge via the Internet at http://pubs.acs.org.

IC051498E